Ferroresonance Suppression by Reinforcing the Capacitance of a Transmission Line

Mohamed Zarouan

Department of Electrical and Computer Engineering, Faculty of Engineering, King Abdulaziz University, P.O. Box 80204, Jeddah 21589, Saudi Arabia
e-mail: mzarouan@kau.edu.sa

Abstract: An electrical network, like any nonlinear system, can have a different steady state response for specific initial conditions basin. An additional battery of capacitors, to be inserted between each phase and the ground, allows to modify the global capacitance of the electrical network which will ensure that the system lies in a domain where the response converges to a unique value. This domain has been determined according to the criterion of stability of Borne and Gentina, applied to the generalized thin arrow form of the power network's state matrix, hereby providing an easy-computable alternative to the complex continuation method.
[Mohamed Zarouan. **Ferroresonance Suppression by Reinforcing the Capacitance of a Transmission Line.** *Life Sci J* 2017;14(8):73-80]. ISSN: 1097-8135 (Print) / ISSN: 2372-613X (Online). http://www.lifesciencesite.com. 11. doi:10.7537/marslsj140817.11.

Keywords: Electrical power network, configuration at risk, coupled phases, continuation method, uniqueness of the response, arrow matrix

1. Introduction

The electrical power networks, often exhibit several steady states, due to the non linearity of their components, which has lead to many works in the literature [1,2,3,4,5,6,7] devoted to the prediction and compensation of the faulty operations. Hence, sufficient conditions of the uniqueness of the response of such systems should be determined.

The funtionning anomaly [8,9,10] of aforementioned system types, and a method which estimates the stability zone of the corresponding deviation system, allowing to derive a condition of uniqueness of its response, were studied previously on by Laurent, Maizieres, Borne, Gentina, Benrejeb, Zarouan etc [11,12,13,14,15,16].

In this paper, the consequences of the onset of a three-phase to earth fault in an electric power network and the possibility to draw a potentially defective configuration are investigated.

The multiplicity of solutions in a three-phase power network, with a potentially defective configuration occurring after the onset of the fault between two phases, is studied in the first part of this paper, using the continuation method applied to the fixed point, based on the Poincaré's map. A domain characterized by the uniqueness of the system's response, related to the absence of operating default, is estimated in the second part, using the stability criterion of Borne and Gentina [14] applied to the deviation system, which characterizes the difference between two responses, related to two distinct initial conditions.

2. The Studied System

The studied system is a three-phase electric power network, corresponding to a set of three voltage transformers VT, which outgoing line comprises several branches, figure 1.

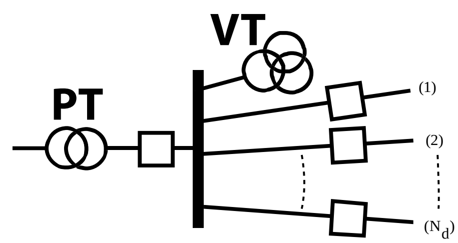

Figure 1: Studied electrical power network.

Because the secondary windings of the power transformer PT, figure 1, are star connected and their common neutral is earthed, the equivalent mono-phase model, figure 2, is sufficient to study and represent a symmetric three-phase network which its phases are uncoupled.

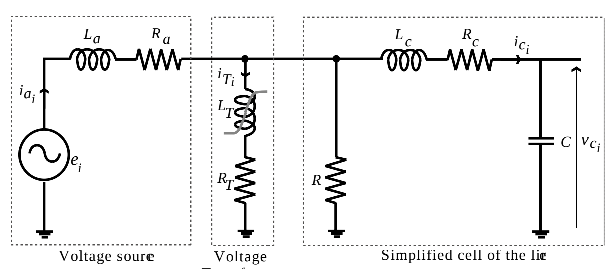

Figure 2: Equivalent model of one phase of the studied electrical network.

Each phase, figure 2, owns a sinusoidal voltage source with amplitude $E = 51kV$, an inductance

$L_a = 1.446H$, and a resistance $R_a = 3.242\Omega$ which account for the series of inductances and resistances located upstream. The model of the line of the studied electrical network merges the outgoing lines in a single cell [5] of phase to ground capacitance $C = 1mF$, line inductance $L_C = 8.978mH$, line resistance $R_C = 0.818\Omega$, and phase to ground resistance $R = 100M\Omega$ which equivalent values are obtained by incorporating the all parameters of the line [16,17,18]. The primary winding of each VT is represented by a resistance $R_T = 118.3\Omega$ put in series with a nonlinear inductance $L_T(i_{T_i})$ [19]. The nonlinear relation binding the current i_{T_i} and the flux ϕ_{T_i} in the winding of the transformer of i^{th} phase is given by the polynomial function in the form (1).

$$i_{T_i} = h(\phi_{T_i}) = a\phi_{T_i} + b\phi_{T_i}^9, i = 1,2,3 \\ a = 1.0024\ 10^{-12} USI \text{ and } b = 1.0095\ 10^{-18} USI \tag{1}$$

A specific study case of a defective electrical network is well-defined and study in this paper. The configuration studied is the fault happened between two phases through the fault conductance G_0 [20]. The equivalent model, figure 3, of this configuration is described by the system of equations (2).

$$\begin{aligned}
\frac{di_{a_i}}{dt} &= -\frac{R_a+R}{L_a} i_{a_i} + \frac{R}{L_a} i_{c_i} + \frac{R}{L_a}\overbrace{\left(a\phi_{T_i} + b\phi_{T_i}^9\right)}^{i_{T_i}} + \frac{1}{L_a} e_i(t) \\
\frac{di_{c_i}}{dt} &= \frac{R}{L_c} i_{a_i} - \frac{R_c+R}{L_c} i_{c_i} - \frac{1}{L_c} v_{c_i} - \frac{R}{L_c}\left(a\phi_{T_i} + b\phi_{T_i}^9\right) \\
\frac{d\phi_{T_i}}{dt} &= Ri_{a_i} - Ri_{c_i} - (R + R_T)\left(a\phi_{T_i} + b\phi_{T_i}^9\right) \\
\frac{dv_{c_i}}{dt} &= \frac{1}{C} i_{c_i} - (2i-3)\frac{G_0}{C}(v_{c_1} - v_{c_2}) \\
e_i(t) &= E \sin\left(\omega t - (i-1)\frac{2\pi}{3}\right), \quad i = 1,2
\end{aligned} \tag{2}$$

3. Fixed Point Diagram

3.1. Coupled Phases Definition

The connection between the two phases through the conductance G_0 is called linear coupling. The interaction between the two phases depends on the value of G_0. If $G_0 = 0\,\Omega^{-1}$ then the two phases are completely coupled and if $G_0 = \infty\,\Omega^{-1}$ then the two phases are completely uncoupled and there is no interaction between them [22,23].

3.2. Symmetry of System - Symmetry of Solution

One of the intrinsic properties of a coupled dynamic system lies in the symmetry which plays a great role in the study of the coupled oscillators. A system in the form (3) is known as symmetric, under the symmetry operation (P_i, θ_i), if it is equivalent to the system (4).

$$\dot{x} = f(x,t), \quad x \in \mathbb{R}^8 \tag{3}$$

$$P_i\dot{x} = f(P_i x, \theta_i(t)), \quad x \in \mathbb{R}^8 \tag{4}$$

P_i is defined by a $n \times n$ transformation matrix, applied to the state variables vector and $\theta_i(t)$ by an transformation of the time variable t.

Only one operation of symmetry, with share identity I_8, could be found in the system (7). The operations of symmetry obtained could be written in the form (5) and can thus be gathered as a set G (6).

$$\begin{aligned}
g_i \quad &: \mathbb{R}^8 \times \mathbb{R} \;\rightarrow\; \mathbb{R}^8 \times \mathbb{R} \\
&(x,t) \;\mapsto\; (P_i x, \theta_i(t)) \\
&i = 1 \ldots k
\end{aligned} \tag{5}$$

$$G = \{(P_i, \theta_i), \quad i = 1 \ldots k, \quad k \in \mathbb{R} \,/\, g_i, \\ \text{is a symetrie operation of (3)}\} \tag{6}$$

$$\bar{I}_8.\pi: (P, \theta(t)) = \left(\begin{bmatrix} -1 & & 0 \\ & \ddots & \\ 0 & & -1 \end{bmatrix}, \omega t - \pi\right) \tag{7}$$

$$G = \{I_8, \bar{I}_8.\pi\} \tag{8}$$

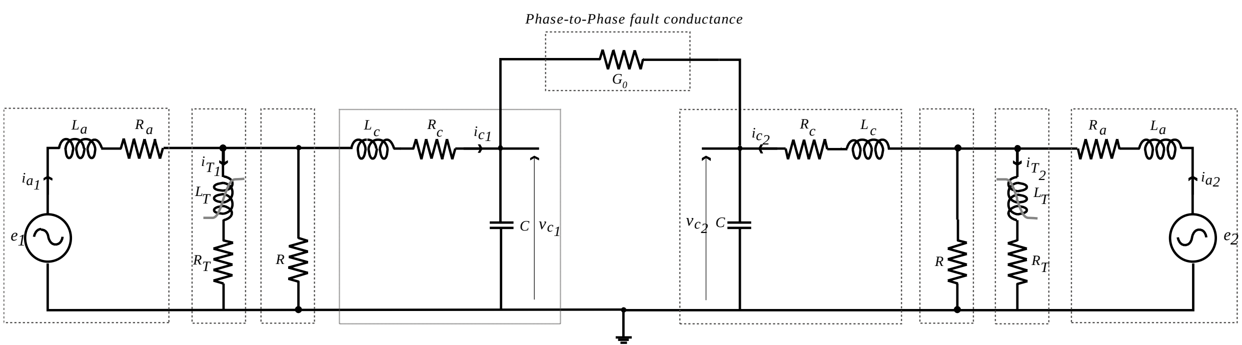

Figure 3: Equivalent model of the new configuration of the studied electrical network.

Since the product of any two of these elements lies in G, G is closed under the product operation. The symmetric group G of is called the Klein 2-group. The periodic solution x is known as completely symmetrical if it is equal to its symmetric element $\bar{x}$ obtained under any symmetry operation (P_i, θ_i), such as $\bar{x} = P_i(x(\theta_i(t)))$. If the periodic solution is invariant only under the change of sign then, as in this studied case, the solution is known as symmetrical by inversion. If the periodic solution is invariant only under the identity operation, then the solution is known as asymmetrical [22].

3.3. Combinatorial Resonances

If each studied phase, separately, exibits a resonant solution, figure 2, then the overall circuit described in figure 3 is likely to be resonant [23].

The i^{th} phase can exhibit the nonlinear resonance with three periodic solutions: non-resonant S_{i1}, resonant S_{i2}, and unstable U_i, $i = 1,2$, figure 4. So, in the two coupled phases, it should exhibit 9 = 3 x 3 combinatorial solutions on weak coupling condition, Table 1. By varying the coupling intensity, the combinatorial resonance exhibits very rich pattern formation behavior, and complicated bifurcations appear, figure 5.

Table 1: Patterns of combinatorial resonances in coupled phases of the studied electrical power network.

S_{11} & S_{21}	U_1 & S_{21}	S_{12} & S_{21}
S_{11} & U_2	U_1 & U_2	S_{12} & U_2
S_{11} & S_{22}	U_1 & S_{22}	S_{12} & S_{22}

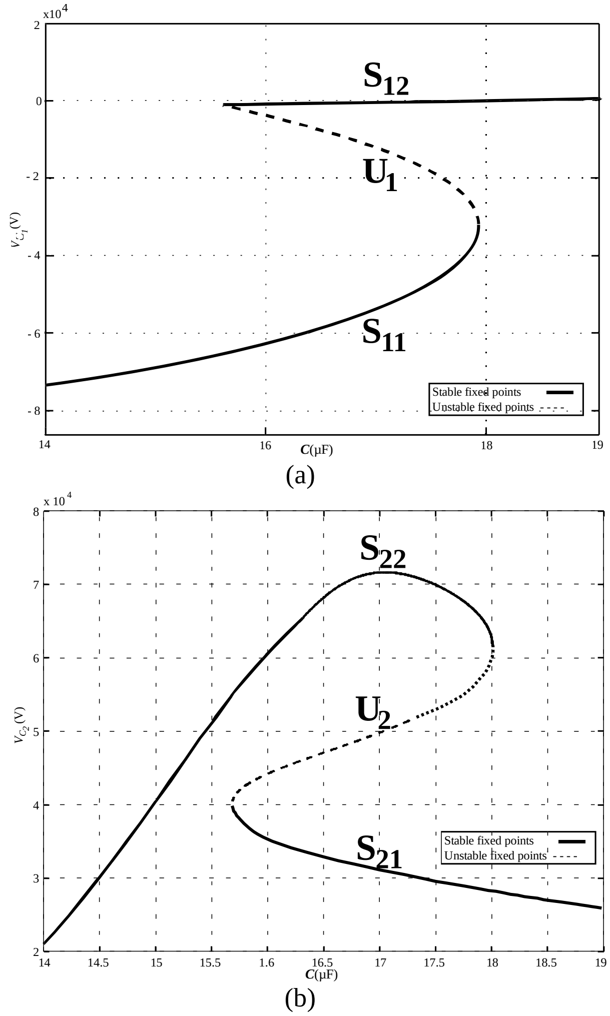

Figure 4: Fixed points diagrams: the first phase (a) is uncoupled with the second phase (b).

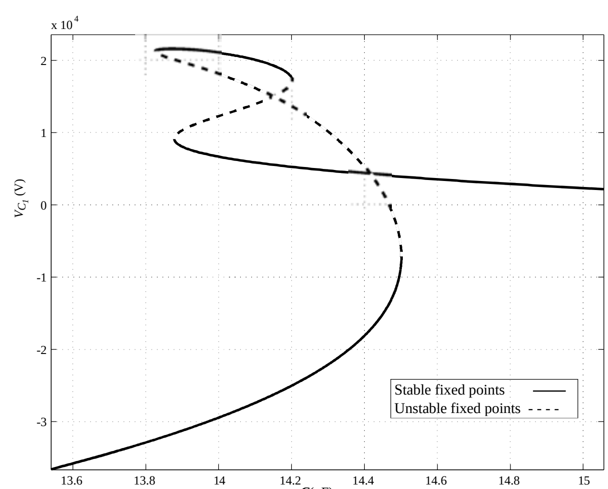

Figure 5: Fixed points diagram of the two coupled phases ($\boldsymbol{G_0 = 2.5\, m\Omega^{-1}}$).

The diagonal of Table 1 showing the nine possible solutions of the global circuit includes three completely symmetrical solutions. The remainder of the elements of the table represents the symmetrical solutions, only obtained by inversion, which shows that all the possible solutions occurring in the studied system are completely symmetrical. Indeed, the global circuit can show, at most, six solutions.

3.4. Results

The model of the studied power network is described in a generic way, by using the notations of equation (9).

$$
\begin{aligned}
&\frac{dx}{dt} = f(t, x, \lambda) \qquad t \in \mathbb{R}, \quad x \in \mathbb{R}^8 \quad et \quad \lambda \in \mathbb{R} \\
&x(t) = \varphi(t, x_0, \lambda) \\
&x = [i_{a_1}, i_{c_1}, v_{c_1}, i_{a_2}, i_{c_2}, v_{c_2}, \phi_{T_1}, \phi_{T_2}]^T \\
&\lambda = C, \quad x(0) = \varphi(0, x_0, \lambda) = x_0
\end{aligned} \tag{9}
$$

The qualitative study of the behavior of a phase, operating independently of the others, has been tackled using the continuation method applied to the fixed point based on the Poincaré's map. Because working out the continuation method needs at least one parameter to be changed, the capacitance C of a phase of the line was chosen to be varied. The two curves in figure 4 prove that the two phases, studied separately, have the same behavior because they have the same number of fold points and the same solution types when the capacitance ranges from $14\,\mu F$ and $19\,\mu F$. The coupling parameter which is the fault conductance between these two phases $G_0 = 2.5\,m\Omega^{-1}$, yields a dynamic behavior, plotted in figure 5, which is a blending, with small distortions, of those in figure 4. Figure 5 represents thus a merging of the two fixed points diagrams which allows to obtain, within a restricted domain, the highest number possible of solutions when the capacitance ranges from $13.6\,\mu F$ and $15\,\mu F$. The maximum number of solutions can decrease to only three solutions if the fault conductance is monitored to $10\,m\Omega^{-1}$ or to $0.5\,m\Omega^{-1}$, figure 6.

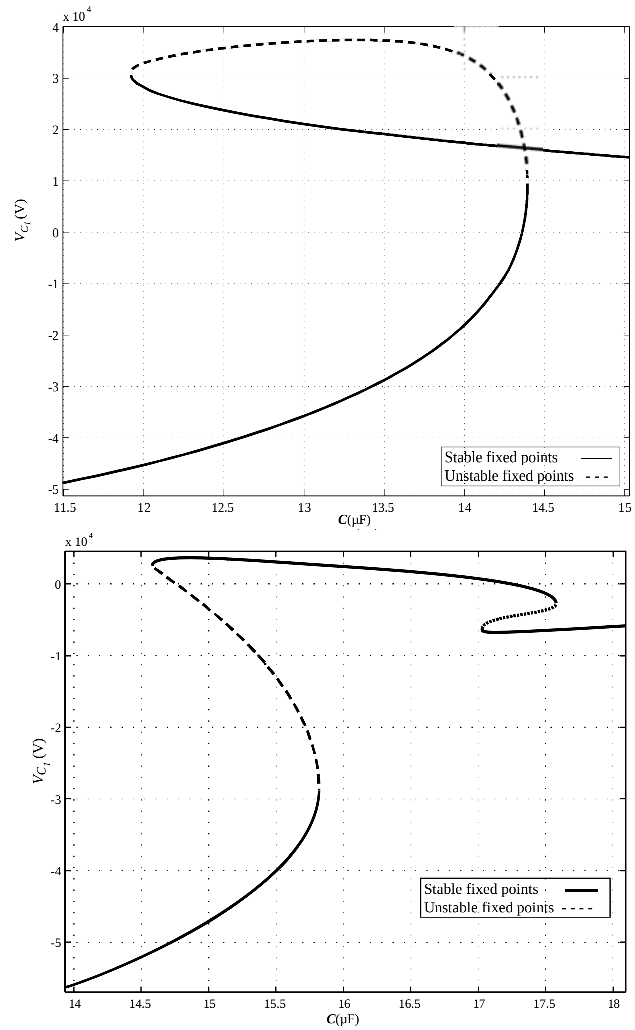

Figure 6: Fixed points diagrams of the two coupled phases circuit (a) $G_0 = 10\,m\Omega^{-1}$ (b) $G_0 = 0.5\,m\Omega^{-1}$.

4. Application of the Criterion of Borne and Gentina for the Search for a Condition of the Uniqueness of the Response

By using the notations of paragraph (3.4), the equations governing the evolution of the network can be reformulated in the state space by (10). The deviation system, which represents the difference between two responses $x^{(1)}$ and $x^{(2)}$ of the studied system subjected to the same inputs but different initial conditions, is described by (11).

$$\dot{x} = \begin{bmatrix} -\frac{R_a+R}{L_a} & \frac{R}{L_a} & 0 & 0 & 0 & 0 & \frac{R}{L_a}(h_1/\phi_{T_1}) & 0 \\ \frac{R}{L_c} & -\frac{R_c+R}{L_c} & -\frac{1}{L_c} & 0 & 0 & 0 & -\frac{R}{L_c}(h_1/\phi_{T_1}) & 0 \\ 0 & \frac{1}{C} & -\frac{G_0}{C} & 0 & 0 & \frac{G_0}{C} & 0 & 0 \\ 0 & 0 & 0 & -\frac{R_a+R}{L_a} & \frac{R}{L_a} & 0 & 0 & \frac{R}{L_a}(h_2/\phi_{T_2}) \\ 0 & 0 & 0 & \frac{R}{L_c} & -\frac{R_c+R}{L_c} & -\frac{1}{L_c} & 0 & -\frac{R}{L_c}(h_2/\phi_{T_2}) \\ 0 & 0 & \frac{G_0}{C} & 0 & \frac{1}{C} & -\frac{G_0}{C} & 0 & 0 \\ R & -R & 0 & 0 & 0 & 0 & -(R+R_T)\,(h_1/\phi_{T_1}) & 0 \\ 0 & 0 & 0 & R & -R & 0 & 0 & -(R+R_T)\,(h_2/\phi_{T_2}) \end{bmatrix} x + \begin{bmatrix} \frac{1}{L_a} & 0 \\ 0 & 0 \\ 0 & 0 \\ 0 & \frac{1}{L_a} \\ 0 & 0 \\ 0 & 0 \\ 0 & 0 \\ 0 & 0 \end{bmatrix} \begin{bmatrix} e_1 \\ e_2 \end{bmatrix} \tag{10}$$

$$\dot{y} = My = \begin{bmatrix} -\frac{R_a+R}{L_a} & \frac{R}{L_a} & 0 & 0 & 0 & 0 & \frac{R}{L_a}h_1^* & 0 \\ \frac{R}{L_c} & -\frac{R_c+R}{L_c} & -\frac{1}{L_c} & 0 & 0 & 0 & -\frac{R}{L_c}h_1^* & 0 \\ 0 & \frac{1}{C} & -\frac{G_0}{C} & 0 & 0 & \frac{G_0}{C} & 0 & 0 \\ 0 & 0 & 0 & -\frac{R_a+R}{L_a} & \frac{R}{L_a} & 0 & 0 & \frac{R}{L_a}h_2^* \\ 0 & 0 & 0 & \frac{R}{L_c} & -\frac{R_c+R}{L_c} & -\frac{1}{L_c} & 0 & -\frac{R}{L_c}h_2^* \\ 0 & 0 & \frac{G_0}{C} & 0 & \frac{1}{C} & -\frac{G_0}{C} & 0 & 0 \\ R & -R & 0 & 0 & 0 & 0 & -(R+R_T)h_1^* & 0 \\ 0 & 0 & 0 & R & -R & 0 & 0 & -(R+R_T)h_2^* \end{bmatrix} y \tag{11}$$

with

$$y = x^{(1)} - x^{(2)}$$

$$h_i^* = \frac{h(\phi_{T_i}^{(1)}) - h(\phi_{T_i}^{(2)})}{\phi_{T_i}^{(1)} - \phi_{T_i}^{(2)}}, \quad i = 1,2$$

The diagonalization by the eigenvector matrix P_A, of the matrix A_{6x6}, upper-left part of the matrix M, gives us D_A (12).

$$D_A = \begin{bmatrix} \lambda_1(C,G_0) & & & & & \\ & \lambda_2(C,G_0) & & & 0 & \\ & & \lambda_3(C,G_0) & & & \\ & & & \lambda_4(C,G_0) & & \\ & 0 & & & \lambda_5(C,G_0) & \\ & & & & & \lambda_6(C,G_0) \end{bmatrix} \tag{12}$$

with $D_A = P_A^{-1}AP_A$.

The evolutions of the real parts of the eigenvalues of A versus to C and G_0 were represented graphically in figure 7.

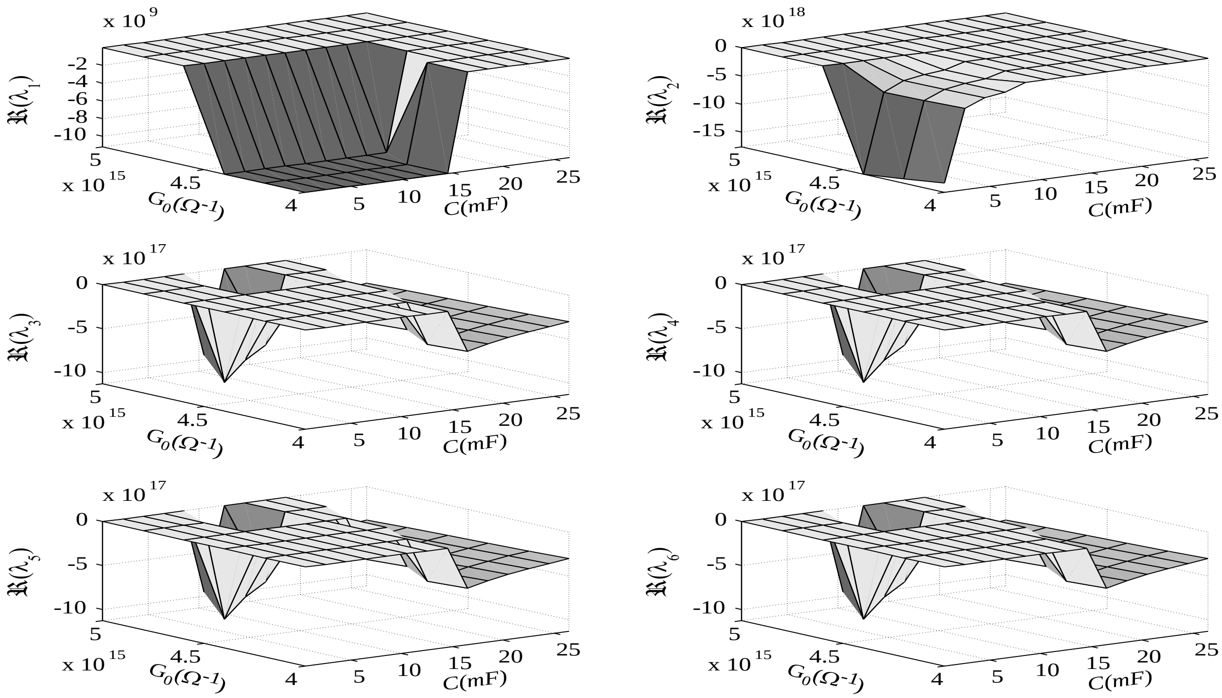

Figure 7: Evaluation of real parts of eigenvalues of A versus $\boldsymbol{C}$ and $\boldsymbol{G_0}$.

The reformulation of the matrix M in the arrow form (13) can be obtained from the following transition matrix P_F,

$$P_F = \begin{bmatrix} & P_A & & 0 & 0 \\ & & & \vdots & \vdots \\ & & & 0 & 0 \\ 0 & \cdots & 0 & 1 & 0 \\ 0 & \cdots & 0 & 0 & 1 \end{bmatrix}$$

with $F = P_F^{-1} M P_F$
yields

$$F = \begin{bmatrix} \lambda_1 & & & F_{1,7}(.) & F_{1,8}(.) \\ & \ddots & & \vdots & \vdots \\ & & \lambda_6 & & \\ F_{7,1} & \cdots & & F_{7,7}(.) & F_{7,8}(.) \\ F_{8,1} & \cdots & & F_{8,7}(.) & F_{8,8}(.) \end{bmatrix} \quad (13)$$

The deviation system, put under this form, becomes $\dot{z} = Fz$. A proof of the asymptotic convergence to zero of the solutions of the system (13) is sufficient to ensure the uniqueness of the response of the network corresponding to the system (11), and thus to provide with a sufficient condition for the system to operate in a non-defective configuration. This condition can be obtained using the criterion of stability of Borne and Gentina [14]. The determination of a comparison system (14) applied to the matrix F (13), based on the hermitian max which is a vector norm, having rank 7, allows to derive a representation in the thin arrow form of the matrix, where all non-constant elements are separated and gathered in only one column. The application of this stability criterion to the matrix $\tilde{F}$ given in (14) can lead to a condition of the uniqueness of the response of the initial system.

$$\tilde{F} = \begin{bmatrix} \Re(\lambda_1) & & & \tilde{F}_{1,7}(.) \\ & \ddots & & \vdots \\ & & \Re(\lambda_6) & \tilde{F}_{6,7}(.) \\ \tilde{F}_{7,1} & \cdots & \tilde{F}_{7,6} & \tilde{F}_{7,7}(.) \end{bmatrix}$$
$$\tilde{F}_{7,i} = \max\left(|F_{7,i}|, |F_{8,i}|\right) \quad (14)$$
$$\tilde{F}_{i,7}(.) = |F_{i,7}(.)| + |F_{i,8}(.)|, i = 1 \ldots 6$$

$$\tilde{F}_{7,7}(.) = \max\begin{pmatrix} \Re\left(F_{7,7}(.)\right) + |F_{7,8}(.)| \\ \Re(F_{8,8}(.)) + |F_{8,7}(.)| \end{pmatrix}$$

Indeed, if the last minor of the matrix $\tilde{F}$ related to the expressions (15) and the chart in figure 8 is negative, then the deviation system (11) is stable and the initial system (10) has the property of uniqueness.

$$\xi_7(C, G_0) = \begin{vmatrix} \Re(\lambda_1) & 0 & 0 & \tilde{F}_{1,7}(.) \\ 0 & \ddots & 0 & \vdots \\ 0 & 0 & \Re(\lambda_6) & \tilde{F}_{6,7}(.) \\ \tilde{F}_{7,1} & \cdots & \tilde{F}_{7,6} & \tilde{F}_{7,7}(.) \end{vmatrix} < 0 \quad (15)$$

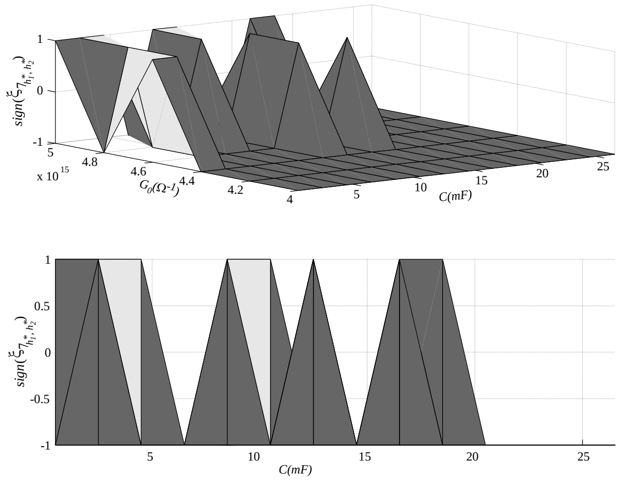

Figure 8: Behavior of the last principal minor of $\widetilde{\boldsymbol{F}}$ versus $\boldsymbol{C}$ and $\boldsymbol{G_0}$.

The functions h_1^* and h_2^* are always positive and depend respectively only on ϕ_{T_1} and ϕ_{T_2}. The value of the minor $\xi_7(C, G_0)$ is negative only if the capacity is higher than $19.5\,mF$. The application of the criterion thus makes it possible to show the uniqueness of the response of the studied power network when the capacitance lies in the zone: $C > 19.5\,mF$.

A rather similar result, in the same way, has been obtained in [24], when the same method was applied for each separate phase, i.e when the conductance G_0 was very small.

5. Conclusion

A practical method, which avoids the multiplicity of responses occurring in an electric power network, is proposed in this paper. The designed compensation method consists of inserting a battery of capacitors between the phase and the ground making it possible to increase the overall capacitance of the circuit to a value for which the response converged towards a unique value. Borne and Gentina stability criterion, applied to deviation system, described by an arrow form characteristic matrix, makes possible to determine a domain of uniqueness of the response, depending on the value of the capacitance C. The efficiency of the proposed method is better than the classical continuation one.

References

1. Jacobson D. Field testing, modelling and analysis of ferroresonance in a high voltage power system. PhD Thesis, The University of Manitoba Winnipeg, Manitoba, Canada, 2000.
2. Milicevic K, Vinko D, Emin Z. Identifying ferroresonance initiation for a range of initial conditions and parameters. Nonlinear dynamics. 2011;66(4):755-62.
3. Amar FB, Dhifaoui R. Study of the periodic ferroresonance in the electrical power networks by bifurcation diagrams. International Journal of Electrical Power Energy Systems. 2011;33(1):61-85.
4. Moses PS, Masoum MA, Toliyat HA. Impacts of hysteresis and magnetic couplings on the stability domain of ferroresonance in asymmetric three-phase three-leg transformers. IEEE Transactions on Energy Conversion. 2011;26(2):581-92.
5. Zarouan M, Ghodbane F, Benrejeb M. Etude de défauts monophasés à la terre dans les réseaux MT. Détection et prévention. Journées scientifiques franco-tunisiennes, Monastir. 2000.
6. Radmanesh H, Gharehpetian GB. Ferroresonance suppression in power transformers using chaos theory. International Journal of Electrical Power Energy Systems. 2013;45(1):1-9.
7. Escudero MV, Dudurych I, Redfern MA. Characterization of ferroresonant modes in HV substation with CB grading capacitors. Electric Power Systems Research. 2007;77(11):1506-13.
8. Rouelle E. Quelques nouvelles expériences de démultiplication de fréquence dans un circuit oscillant dont la bobine est à noyau de fer. Rev.. de I'Elec. 1936;40:811-9.
9. Dehors R. Recherches sur la démultiplication de Fréquence Ferromagnétique. Revue Générale de l'Electricite. 1947:455-67.
10. Dehors R. Contribution à l'étude de la démultiplication de fréquence ferromagnétique. In: Annales de Physique 1946;11(1):607-720.
11. Laurent F, Vidal P. Sur une condition suffisante d'unicité de la réponse d'un système échantillonné non linéaire à une sollicitation quelconque. CRAS. 1967;264(A):779.
12. Maizières C. Sur quelques méthodes d'étude des systèmes continus non linéaires. Doct. Dissertation In physiques. Lille. 1968.
13. Borne P, Benrejeb M. On the stability of a class of interconnected systems. Applications to the forced working conditions. In: Multivariable Technological Systems: Proceedings of the Fourth IFAC International Symposium. Fredericton, Canada.,4-8 July 1977, p. 261.
14. Gentina J.C, Borne P, Laurent F. Maizières C. Sur une condition suffisante d'unicité de la réponse des systèmes continus non linéaires de grandes dimension. RAIRO. 1972:3(1).
15. Benrejeb M. Synchronisation des systèmes continus non-lináires en régime forcé, Thèse de

Docteur Ingénieur, UST-Lille, 1976.
16. Zarouan M, Allali S, Benrejeb M. Correlation between the bifurcation diagram structure and the predominant harmonics of an electrical power network response. Chaos, Solitons & Fractals. 2009 Oct 15;42(1):483-91.
17. Zarouan M. Sur le comportement complexe de systèmes non linèaires. Cas de réseaux d'énergie électrique en régime de défauts. Ph. D. Thesis, ENI-Tunis, 2007.
18. Kirtley JL. Electric power principles: sources, conversion, distribution and use. John Wiley Sons; 2011 Jul 5.
19. Lopez-Fernandez XM, Ertan HB, Turowski J. Transformers: analysis, design, and measurement. CRC. 2012.
20. Raison B, Chilard O, Penkov D, Pham DC. Protection, detection and isolation of faults in MV Networks in the presence of decentralized production. Electrical Distribution Networks. 2011:351-94.
21. Kawakami H. Bifurcation of periodic responses in forced dynamic nonlinear circuits, computation of bifurcation values of the system parameters. IEEE Transactions Circuits and Systems. 1984;31(3):248-60.
22. Lin Y. Periodic oscillation analysis for a coupled FHN network model with delays. In: Abstract and Applied Analysis. Hindawi Publishing Corporation. 2013;2013(1):1-6.
23. Kawakami H. Combinatorial resonances in a coupled Duffing’s circuit with asymmetry. IEICE Transactions on Fundamentals of Electronics, Communications and Computer Sciences. 2003;86(9):2340-6.
24. Zarouan M, Dieulot JY, Benrejeb M. Sur l’unicité de la réponse d’un réseau d’énergie électrique en régime de défauts, Revue des Sciences et Technologies de l’Automatique e-STA. 2006;9(4):1-6.

8/25/2017